When Are Asymmetric Fixed-Effects Models Within-Person Tests of Reversibility? Heterogeneous Responses and Bidirectional Support*

Jiwon Lee†

August 29, 2026

Abstract

Asymmetric fixed-effects models are increasingly used in sociological research to test whether an effect reverses when a time-varying predictor changes direction. Because these models rely on within-person change, directional asymmetry is often interpreted as evidence of within-person irreversibility. This study shows that this interpretation requires an additional cross-person homogeneity assumption. I reparameterize Allison's (2019) cumulative asymmetric fixed-effects model exactly as a model of current state and total movement, revealing that the specification pools current-state responses across individuals. When those responses are heterogeneous and systematically related to who moves upward versus downward, pooled asymmetry can arise even when every individual's response is perfectly reversible. I derive this mover-composition result and characterize what remains identifiable when individual state responses are unrestricted. A common path response—the additional response associated with accumulated movement conditional on current state—can then be identified only from within-person bidirectional movement, provided that the resulting variation is not absorbed by period effects. Monte Carlo simulations and a reanalysis of Allison's wage example illustrate the resulting assumption–support–precision trade-off and show that relevant support depends on the structure of observed trajectories, not simply on the number of directional transitions.

Keywords: fixed effects; asymmetric fixed-effects models; panel data; directional asymmetry; path dependence.

*I thank Sungsik Hwang for an early conversation that first prompted my interest in asymmetric fixed-effects models. During preparation of the manuscript, ChatGPT 5.6 Sol (OpenAI) and Claude Fable 5 (Anthropic) were used to verify mathematical derivations and code, assist in developing and generalizing selected technical details, and support occasional editing. The author reviewed and revised all AI-assisted output and takes full responsibility for the manuscript, including the accuracy of its analyses and citations.

† Postdoctoral Fellow, Cornell Population Center, Cornell University, Ithaca, NY, USA. Email: jiwon.lee@cornell.edu.

1. Introduction

Many sociological arguments involve claims about whether social processes are reversible (Lieberson 1985). A spell of unemployment may leave a wage scar after reemployment (Gangl 2006); incarceration may alter later earnings even after release (Western 2002); and cumulative-advantage processes may leave residues that current status alone cannot summarize (DiPrete and Eirich 2006). In each case, a movement into a state and a later movement out of it need not retrace the same outcome path. Asymmetric panel models are attractive because they let researchers ask whether increases and decreases in a time-varying predictor have equal and opposite consequences.

In sociology, York and Light (2017) proposed a general strategy for estimating directional asymmetry, and Allison (2019) developed the approach for short panels, generalized linear models, and multiperiod settings. Related positive/negative partial-sum decompositions appear in energy-demand and nonlinear time-series models (Gately and Huntington 2002; Shin et al. 2014). Applications are rapidly increasing in sociology and other disciplines, now spanning environmental sociology (Clement and York 2017; Huang and Jorgenson 2018; York 2012), social roles and mental health (Mize and Kincaid 2025), spousal caregiving (Uccheddu et al. 2019), health and fertility expectations (Lazzari and Beaujouan 2025), procedural justice and legitimacy (Thompson and Pickett 2021), and psychotherapy processes (Sun et al. 2021). In these applications, the directional contrast is often interpreted substantively as evidence about whether a process fully reverses when the predictor changes direction.

Fixed-effects (FE) estimation seems especially well suited to this task. FE transformations remove stable unit-specific differences in outcome levels and evaluate changes in the predictor within the same unit (Allison 2009; Firebaugh et al. 2013; Halaby 2004). It is therefore tempting to reason that if increases and decreases are both estimated from within-person change, their difference is itself a within-person comparison of what happens when a process runs forward versus backward.

This study shows that the last step need not follow. *The change underlying each directional coefficient can be within-person even when the contrast between the directional coefficients is supplied by different people.* If individuals differ in how strongly their outcomes respond to the current state of the predictor, and those response functions differ systematically between people observed moving upward and people observed moving downward, a pooled asymmetric FE model can report directional asymmetry even when every individual's response is perfectly reversible. Therefore, fixed effects remove stable heterogeneity in outcome levels; they do not, by themselves, remove stable heterogeneity in response slopes.

To make this issue visible, I first rewrite Allison's cumulative asymmetric model using an exactly equivalent parameterization. Cumulative positive and negative changes encode two quantities: their difference is net change from baseline, or the predictor's endpoint relative to where it began, whereas their sum is total movement, the cumulative amount of movement in either direction. Allison's model can therefore be expressed in terms of current state and accumulated movement. Under this representation, the usual symmetry restriction implies that total movement has no additional association with the outcome conditional on current state. Directional asymmetry is thus a limited form of history dependence: trajectories reaching the same state can imply different outcomes if they accumulated different amounts of movement along the way.

The reparameterization also makes visible what must be pooled across people. The pooled asymmetric FE specification constrains the current-state response to be common across individuals who contribute upward and downward movements. That restriction may be reasonable and, when correct, lets the pooled estimator use individuals who move in only one direction. But it becomes consequential when the claim concerns *individual-level reversibility*. If current-state responses differ systematically between upward and downward movers, the pooled path response combines genuine path dependence with mover composition. In a two-wave binary panel, the latter equals half the difference between the groups' average current-state responses, so the pooled path response can be nonzero even when every individual's path response is zero. This raises a natural identification question: what remains identifiable if this cross-person restriction is relaxed?

I address this question by allowing each individual to have an unrestricted stable current-state response and asking what variation remains to identify a common path response. Once individual state responses are absorbed, individuals who move only upward or only downward cannot separate the state response from the path response because signed and absolute change are perfectly collinear. The needed separation comes from individuals observed moving in both directions. The clearest case is a person who moves away from an initial state and later returns to it: the same person's state response operates with opposite signs across the two movements and can cancel, leaving variation that distinguishes a common path response. With two waves, no individual can move in both directions, so this separation is impossible without reimposing cross-person comparability.

The study makes three contributions. First, it identifies an estimand problem in pooled asymmetric FE models. The exactly equivalent state–path representation shows that heterogeneous current-state responses can generate pooled directional asymmetry even when every individual's response is fully reversible. Second, it characterizes identification after relaxing the common-state-response restriction. With stable individual differences in state response left unrestricted, a common path response requires within-person movement in both directions, together with a global rank condition requiring that the resulting variation survive adjustment for period effects. Third, it translates these results into an applied assumption–support–precision trade-off.

The pooled estimator is a parsimonious baseline when common state responses are credible and can be more precise when bidirectional support is sparse; the heterogeneous-state-response specification provides a sensitivity or primary analysis when cross-person comparability is doubtful. Monte Carlo simulations and a reanalysis of Allison's (2019) wage example show how these choices interact with the trajectory structure observed in practice.

The remainder of the study proceeds as follows. Section 2 develops the state–path representation of asymmetric FE models. Section 3 shows how heterogeneous state responses can generate apparent irreversibility. Section 4 derives the bidirectional-support result and the heterogeneous-state-response estimator. Section 5 translates the theory into a practical workflow for applied researchers and clarifies the scope of causal interpretation. Sections 6 and 7 provide Monte Carlo and empirical illustrations. Section 8 concludes.

2. Asymmetric Fixed Effects as a Model of State and Path

Asymmetric models allow the effect of a change in a predictor to depend on its direction, an idea appearing in sociological discussions of irreversibility (Lieberson 1985), economic models of "imperfect reversibility" (Gately and Huntington 2002), and nonlinear time-series models based on positive and negative partial sums (Shin et al. 2014). York and Light (2017) adapted this logic to sociological panel models, Allison (2019) developed a cumulative asymmetric FE specification for multiperiod data, and Arita (2022) relaxed the same restriction in a first-difference framework. I begin with Allison's formulation and show that it admits an exactly equivalent representation in terms of current state and total movement.

Consider individuals $i = 1, \ldots, N$ observed at waves $t = 1, \ldots, T_i$, with outcome Y_{it} and time-varying predictor X_{it}. Write $\Delta Y_{it} = Y_{it} - Y_{i,t-1}$ and $\Delta X_{it} = X_{it} - X_{i,t-1}$. With two waves, Allison's asymmetric first-difference model is

$$\Delta Y_i = \delta + \beta_+ \Delta X_i^+ + \beta_- \Delta X_i^- + u_i, \tag{1}$$

where

$$\Delta X_i^+ = \max(\Delta X_i, 0), \qquad \Delta X_i^- = \max(-\Delta X_i, 0).$$

In Equation (1), β_+ is the outcome change associated with a one-unit increase in X, while β_- is the outcome change associated with a one-unit decrease; δ is a common intercept absorbing the period effect, and u_i is an idiosyncratic error. Directional symmetry is

$$H_0: \ \beta_+ = -\beta_-. \tag{2}$$

For more than two observations, Allison proposes a cumulative specification. Define cumulative positive and negative movement by

$$Z_{it}^{+} = \sum_{s=2}^{t} \Delta X_{is}^{+}, \qquad Z_{it}^{-} = \sum_{s=2}^{t} \Delta X_{is}^{-}.$$

with the empty-sum convention $Z_{i1}^{+} = Z_{i1}^{-} \equiv 0$. The model is

$$Y_{it} = \alpha_i + \lambda_t + \beta_{+} Z_{it}^{+} + \beta_{-} Z_{it}^{-} + \epsilon_{it}, \tag{3}$$

where α_i and λ_t are unit and period effects. For binary X, Z_{it}^{+} counts entries into the state and Z_{it}^{-} counts exits; for continuous X, they accumulate the magnitudes of positive and negative movements. Past movements therefore remain encoded in the outcome through the cumulative sums.

2.1. An exact state–path representation

The cumulative positive and negative movements can be reexpressed as two alternative summaries of the same exposure history. Define net displacement as

$$D_{it} = Z_{it}^{+} - Z_{it}^{-}$$

and total movement as

$$V_{it} = Z_{it}^{+} + Z_{it}^{-} = \sum_{s=2}^{t} |\Delta X_{is}|.$$

Thus $V_{i1} \equiv 0$ under the same empty-sum convention.

By telescoping,

$$D_{it} = X_{it} - X_{i1}.$$

It follows that

$$Z_{it}^{+} = \frac{V_{it} + D_{it}}{2}, \qquad Z_{it}^{-} = \frac{V_{it} - D_{it}}{2}.$$

Substituting these expressions into Equation (3) and absorbing the time-invariant term involving X_{i1} into the unit effect (so that $\alpha_i^{*} = \alpha_i - \theta X_{i1}$) gives

$$Y_{it} = \alpha_i^{*} + \lambda_t + \theta X_{it} + \phi V_{it} + \epsilon_{it}, \tag{4}$$

where

$$\theta = \frac{\beta_+ - \beta_-}{2}, \qquad \phi = \frac{\beta_+ + \beta_-}{2}, \tag{5}$$

with inverse mapping

$$\beta_+ = \theta + \phi, \qquad \beta_- = -\theta + \phi.$$

Section A of the Online Supplement gives the algebra in full. The directional and state–path formulations are exactly equivalent: they generate the same fitted values and likelihood and differ only in parameterization. Separate responses to positive and negative movement may suggest a different sociological process from a current-state response plus cumulative path dependence, but within this specification the data cannot distinguish these interpretations.

The state–path representation makes the substantive content of the cumulative model more transparent. Net displacement records where X stands relative to its starting value, whereas V_{it} records how much movement occurred along the way. For a binary predictor, for example, the histories $(0, 0, 0)$ and $(0, 1, 0)$ have the same starting and ending states but total movement of zero and two, respectively. Equation (4) therefore assigns them an exposure-history difference of 2ϕ. In a marital-status application with log wages as the outcome, θ captures the association with current marital status, while ϕ captures the additional association with accumulated marital transitions conditional on current status.

This representation also clarifies the symmetry restriction in Equation (2):

$$\beta_+ = -\beta_- \quad \Longleftrightarrow \quad \phi = 0.$$

Within the maintained cumulative specification, directional symmetry is therefore equivalent to a zero path response, $\phi = 0$. I refer to ϕ throughout as the *path response*. A nonzero path response represents a restricted form of path dependence within the state–total-movement model: histories reaching the same current state may differ in expected outcomes because they accumulated different amounts of total movement. The model cannot distinguish histories that differ in timing, duration, ordering, or other features while producing the same endpoint and total movement.

The value of the state–path representation for the present analysis is diagnostic. It separates the current-state response, θ, from the path response, ϕ, and thereby makes explicit that the pooled asymmetric FE model imposes a common θ across individuals. The next question is what happens when that restriction is relaxed: can the path response still be distinguished from heterogeneous individual responses to the current state? The next section shows that the answer depends on who supplies the upward and downward movements observed in the panel.

3. Why Pooled Asymmetry Need Not Be Individual-Level Asymmetry

Equation (4) absorbs arbitrary stable differences in outcome levels through α_i but imposes a common current-state response θ. To see what the pooled asymmetric FE estimator represents when this restriction fails, allow both the state and path responses to vary across individuals:

$$Y_{it} = \alpha_i + \lambda_t + \theta_i X_{it} + \phi_i V_{it} + \epsilon_{it}. \tag{6}$$

This formulation lets us decompose the pooled directional contrast into two components: variation attributable to individual path responses and variation arising from heterogeneity in current-state responses. When the individuals supplying upward movements have systematically different θ_i from those supplying downward movements, the latter component can generate pooled asymmetry even if $\phi_i = 0$ for every individual. In other words, the pooled model may indicate irreversibility even when each individual's response is fully reversible.[1]

3.1. The two-wave binary case

The estimand problem is easiest to see with a binary predictor and two waves. Let $X \in \{0, 1\}$, and define $G_i^+ = 1$ for an upward mover $(0 \to 1)$, $G_i^- = 1$ for a downward mover $(1 \to 0)$, and $G_i^0 = 1$ for a stayer. First differencing Equation (6) yields

$$\Delta Y_i = \delta + \theta_i \Delta X_i + \phi_i |\Delta X_i| + u_i.$$

The three possible transition types therefore satisfy

$$\begin{aligned} 0 \to 1: &\quad \Delta Y_i = \delta + \theta_i + \phi_i + u_i, \\ 1 \to 0: &\quad \Delta Y_i = \delta - \theta_i + \phi_i + u_i, \\ \text{stayer}: &\quad \Delta Y_i = \delta + u_i. \end{aligned}$$

Under $E(u_i \mid G_i^+, G_i^-, G_i^0) = 0$, a regression with an intercept and separate indicators for upward and downward movement is saturated across the three transition categories. Its population directional coefficients are therefore

$$\beta_+^* = E(\theta_i + \phi_i \mid G_i^+ = 1), \qquad \beta_-^* = E(-\theta_i + \phi_i \mid G_i^- = 1).$$

[1] This issue is related to, but distinct from, the slope-heterogeneity problem studied by Thombs et al. (2022). They examine the behavior of pooled FE estimators under heterogeneous slopes in large-N, large-T dynamic panels and motivate heterogeneous-panel estimators. The concern here is instead with what the pooled directional contrast represents when opposite directions are supplied by individuals with different current-state responses, including in short panels where individual directional effects cannot be estimated.

Applying the transformation in Equation (5) gives

$$\phi^*_{\text{pool}} = \frac{\beta^*_+ + \beta^*_-}{2} \tag{7}$$

$$= \underbrace{\frac{E(\phi_i \mid G_i^+ = 1) + E(\phi_i \mid G_i^- = 1)}{2}}_{\text{direction-specific path component}} + \underbrace{\frac{E(\theta_i \mid G_i^+ = 1) - E(\theta_i \mid G_i^- = 1)}{2}}_{\text{mover-composition term}}. \tag{8}$$

Equation (8) shows that the pooled path response contains not only the average path responses among upward and downward movers, but also any difference in current-state responses between the two groups. Consequently, pooled directional asymmetry need not reflect individual-level path dependence.

The implication is sharpest under universal individual-level reversibility. Suppose

$$\phi_i = 0 \qquad \text{for every } i.$$

Each individual's response is then exactly reversible: an upward change has response $\beta_{i+} = \theta_i$, while an equal downward change has response $\beta_{i-} = -\theta_i$. Nevertheless,

$$\phi^*_{\text{pool}} = \frac{E(\theta_i \mid G_i^+ = 1) - E(\theta_i \mid G_i^- = 1)}{2}. \tag{9}$$

Equation (9) shows that universal individual-level symmetry is fully compatible with pooled directional asymmetry whenever upward and downward movers differ in their average current-state responses.

A simple example illustrates the distinction. Suppose X indicates marriage and Y is log wages. Among people observed entering marriage, let the average marriage response be .04; among those observed leaving marriage, let it be 0.02. Suppose further that $\phi_i = 0$ for everyone, so each person's wage response is perfectly reversible: entering marriage adds that individual's marriage premium, and leaving marriage removes exactly the same amount. The pooled directional coefficients are nevertheless $\beta^*_+ = 0.04$, $\beta^*_- = -0.02$, which imply $\phi^*_{\text{pool}} = 0.01$. Under the state–path interpretation, a marriage–divorce sequence would therefore be assigned a log-wage residue of $2\phi^*_{\text{pool}} = 0.02$, or approximately 2 percent. Yet no individual in the data-generating process has any such residue. It arises entirely because the upward coefficient averages the responses of one group of people and the downward coefficient averages the responses of another.

Fixed effects do not remove this source of heterogeneity. If the true reversible model is

$$Y_{it} = \alpha_i + \lambda_t + \theta_i X_{it} + \epsilon_{it},$$

then first differencing removes the unit-specific level α_i but leaves

$$\Delta Y_{it} = \delta_t + \theta_i \Delta X_{it} + \Delta\epsilon_{it},$$

where $\delta_t = \lambda_t - \lambda_{t-1}$ is the differenced period effect. FE estimation therefore eliminates stable heterogeneity in outcome levels, not stable heterogeneity in responses to X. Thus, *each directional coefficient may be estimated from within-person change even though the contrast between them need not compare opposite movements within the same person's response function*.[2]

With longer panels, the same logic extends beyond simple averages. The pooled coefficient becomes a design-weighted projection in which the direction, magnitude, frequency, and timing of each individual's movements determine how heterogeneous θ_i and ϕ_i enter the estimand. Section B of the Online Supplement gives the general multiperiod expression. For the argument here, the implication is unchanged: observing upward and downward movements somewhere in the panel does not ensure that their contrast compares opposite movements within the same individual response function.

4. Identifying a Common Path Response without a Common State Response

The previous section showed that pooled directional asymmetry can reflect differences in current-state responses between the people supplying upward and downward movements. This raises a natural identification question: what can identify a common path response if individuals are allowed to have different stable current-state responses?

To answer this question, consider a specification that leaves each individual's stable state response unrestricted while retaining a common path response:

$$Y_{it} = \alpha_i + \lambda_t + \theta_i X_{it} + \phi V_{it} + \epsilon_{it}. \tag{10}$$

Here the θ_i are unrestricted nuisance parameters, while ϕ retains the same interpretation as in the state–path representation: it captures the association with accumulated movement conditional on current state. Relative to the pooled asymmetric model, Equation (10) relaxes the cross-person restriction on state responses while continuing to pool the path response across individuals. This removes the mover-composition term identified in Section 3, but it necessarily demands stronger within-person support for ϕ. I refer to Equation (10) as the

[2] An analogous composition issue appears in the econometric literature on two-way fixed-effects models with heterogeneous treatment effects. In that setting, pooled estimators may combine the effects of units entering and leaving treatment with nonconvex weights (de Chaisemartin and D'Haultfœuille 2020). The present problem differs in that rather than asking whether a pooled coefficient recovers a meaningful average causal effect, I ask whether asymmetry between directional coefficients can be interpreted as evidence that the same response process is irreversible.

heterogeneous-state-response (HSR) specification.

First differencing yields

$$\Delta Y_{it} = \delta_t + \theta_i \Delta X_{it} + \phi |\Delta X_{it}| + u_{it}, \tag{11}$$

where $\delta_t = \lambda_t - \lambda_{t-1}$, as before, and $u_{it} = \epsilon_{it} - \epsilon_{i,t-1}$. Because V_{it} cumulates absolute changes, $\Delta V_{it} = |\Delta X_{it}|$, so the first-difference path regressor is absolute change. The identification problem is now transparent. Signed change, ΔX_{it}, is allowed to have an individual-specific coefficient, so absolute change, $|\Delta X_{it}|$, can identify ϕ only to the extent that it contains variation not already explained by individual-specific signed change and period effects. The remainder of this section characterizes when such residual variation exists.

4.1. Bidirectional support

To isolate the within-person support condition, first suppose that common period effects have been partialled out. For individual i, stack the $T_i - 1$ observed changes as

$$\mathbf{d}_i = (\Delta X_{i2}, \ldots, \Delta X_{iT_i})', \qquad \mathbf{a}_i = (|\Delta X_{i2}|, \ldots, |\Delta X_{iT_i}|)'.$$

The vector $\mathbf{d}_i$ records signed changes, while $\mathbf{a}_i$ records absolute changes. For any symmetric positive-definite weighting matrix W_i and any individual with $\mathbf{d}_i \neq \mathbf{0}$, define the weighted residual-maker

$$M_{d_i}^{W_i} = I - \mathbf{d}_i(\mathbf{d}_i' W_i \mathbf{d}_i)^{-1} \mathbf{d}_i' W_i,$$

and the residual variation in absolute change

$$w_i(W_i) = \mathbf{a}_i' W_i M_{d_i}^{W_i} \mathbf{a}_i.$$

For individuals with no change in X, set $w_i(W_i) = 0$. Thus $w_i(W_i)$ is the residual variation in absolute movement after removing the individual's signed movement.

Proposition 1 (Weighting-invariant bidirectional support)**.** *For any symmetric positive-definite W_i, $w_i(W_i) > 0$ if and only if individual i experiences at least one positive and at least one negative nonzero change in X over the observed panel.*

Section C of the Online Supplement gives the proof. The intuition follows from $\mathbf{a}_i = |\mathbf{d}_i|$ elementwise. If all nonzero changes are upward, $\mathbf{a}_i = \mathbf{d}_i$; if all are downward, $\mathbf{a}_i = -\mathbf{d}_i$. Absolute and signed change are then perfectly proportional and the unrestricted θ_i absorbs the path regressor. Movement in both directions

A. Cross-person opposite directions

$$i:\ 0 \xrightarrow{\theta_i + \phi} 1$$

$$j:\ 1 \xrightarrow{-\theta_j + \phi} 0$$

combined response $= 2\phi + (\theta_i - \theta_j)$

B. Within-person reversal

$$i:\ 0 \xrightarrow{\theta_i + \phi} 1 \xrightarrow{-\theta_i + \phi} 0$$

combined response $= 2\phi$

Figure 1: Cross-person directional contrast and within-person reversal

breaks this proportionality, regardless of the positive-definite weighting scheme.

The binary reversal $0 \to 1 \to 0$ gives the clearest illustration. Under Equation (10), the upward and downward transition responses for the same individual are $\theta_i + \phi$ and $-\theta_i + \phi$. Summing them gives

$$(\theta_i + \phi) + (-\theta_i + \phi) = 2\phi,$$

so the individual's stable state response cancels. If the opposite directions instead come from different individuals i and j, their combined response is

$$(\theta_i + \phi) + (-\theta_j + \phi) = 2\phi + (\theta_i - \theta_j),$$

and the cross-person difference in state responses remains. Bidirectional movement within the same individual is what removes this mover-composition term. Figure 1 illustrates the distinction.

Under identity weighting, the amount of such within-person support has a simple closed form. Define

$$S_i^+ = \sum_{t:\Delta X_{it}>0} (\Delta X_{it})^2, \qquad S_i^- = \sum_{t:\Delta X_{it}<0} (\Delta X_{it})^2.$$

For $S_i^+ + S_i^- > 0$,

$$w_i(I) = \frac{4S_i^+ S_i^-}{S_i^+ + S_i^-}. \tag{12}$$

Section C of the Online Supplement gives the derivation. The measure is zero when either direction is absent and increases as squared movement accumulates in both directions. For binary X, S_i^+ and S_i^- reduce to the numbers of entries and exits, respectively. Thus the relevant support depends not simply on how often X changes, but on how much movement in both directions occurs within the same individual.

An exact return to the starting point is sufficient but not necessary. With a continuous predictor, for example, the trajectory $0 \to 3 \to 1$ contains signed changes $(3, -2)$ and absolute changes $(3, 2)$. These vectors are not proportional, so total movement contains variation beyond the individual's signed changes even though the endpoint differs from the starting value. The identifying requirement is therefore bidirectional movement, not a completed return to baseline.

4.2. Two waves cannot provide within-person directional comparison

Proposition 1 yields an immediate implication for two-wave asymmetric FE designs. With only one observed change per individual, no person can contribute movement in both directions. For a mover, $|\Delta X_i|$ is therefore perfectly proportional to ΔX_i; for a stayer, both are zero. The pooled asymmetric FE model can nevertheless estimate separate upward and downward coefficients because it combines changes from different mover populations under a common state-response parameter. Once θ_i is left unrestricted, that cross-person pooling can no longer separate state response from path response. A two-wave panel can therefore show that upward and downward movers experience different average outcome changes, but without additional response-homogeneity assumptions it cannot determine whether the same individual's response would differ when the direction of change is reversed.

4.3. Global rank and estimation

Within-person bidirectional support is necessary but not sufficient for identification in the full model. Common period effects may absorb the absolute-change variation that remains after individual-specific state responses are removed. Stack Equation (11) as

$$\mathbf{y} = \mathbf{D}\boldsymbol{\delta} + \mathbf{Z}\boldsymbol{\theta} + \phi\mathbf{a} + \mathbf{u},$$

where $\mathbf{D}$ contains period-difference indicators, $\mathbf{Z}$ contains the individual-specific signed-change regressors, and $\mathbf{a}$ stacks $|\Delta X_{it}|$. Let $\mathbf{A} = [\mathbf{D}, \mathbf{Z}]$, and let M_A^W denote the weighted residual-maker for the nuisance space spanned by $\mathbf{A}$. Under any positive-definite weighting matrix W, ϕ is identified if and only if

$$\mathbf{a}' W M_A^W \mathbf{a} > 0. \tag{13}$$

Bidirectional movement is therefore necessary but not sufficient in the full model: the residual absolute-change variation generated within individuals must also survive the common-period projection. If everyone follows the same $0 \to 1 \to 0$ trajectory at the same dates, for example, absolute change is period-specific and is absorbed by the period effects; staggered reversals or reversers observed alongside stayers can preserve the required variation. Individuals without bidirectional histories may affect this global projection through common nuisance parameters, but they do not themselves supply direct within-person separation of signed and absolute movement. Section C of the Online Supplement gives additional rank examples.

Estimation follows directly from Equation (10). In levels, the HSR specification includes unit and period effects, individual-specific slopes on X_{it}, and a common coefficient on V_{it}. Equivalently, Frisch–Waugh–Lovell partialling (Frisch and Waugh 1933; Lovell 1963) residualizes the outcome and V_{it} against the full nuisance space before estimating ϕ; existing varying-slope fixed-effects methods can implement this directly (Rüttenauer and Ludwig 2023).

The pooled and HSR specifications therefore embody an assumption–support–precision trade-off. The pooled estimator assumes a common state response and can use unidirectional movers, which may improve precision when bidirectional support is sparse. HSR removes that cross-person comparability restriction but learns ϕ from the residual variation that remains after individual state responses are absorbed. Precision can consequently deteriorate when that variation is limited or concentrated.

5. A Practical Workflow for Assessing Reversibility

The identification results clarify what researchers should establish before interpreting pooled directional asymmetry as evidence about individual-level reversibility. Observing both directions somewhere in the sample is sufficient only under a cross-person comparability restriction on current-state responses. Once that restriction is relaxed, the relevant questions are *who supplies those directions* and whether residual identifying variation survives the nuisance structure of the intended model.

For a binary predictor, a basic support audit should classify individuals into four groups: no transition, entry only, exit only, and both entry and exit. Only the last group supplies direct within-person bidirectional movement capable of separating a common path response from unrestricted stable state-response heterogeneity. Researchers should report the number of such individuals and the timing and frequency of their transitions. For a continuous predictor, S_i^+, S_i^-, and Equation (12) quantify the same support, while Equation (13) indicates whether it survives adjustment for period effects. For discrete predictors, researchers should also inspect whether a small number of apparent reversals could plausibly reflect measurement error.

A practical analysis can then proceed in three stages. First, estimate the pooled asymmetric FE model and translate its directional coefficients into the equivalent state–path parameters (θ, ϕ). Second, audit bidirectional and global support to determine whether the common-state-response restriction can be relaxed in the observed panel. Third, when meaningful residual support remains, estimate Equation (10) as a sensitivity analysis, or as the primary specification when a common current-state response is substantively difficult to defend. Differences between $\hat{\phi}_{\text{pool}}$ and the HSR estimate can be informative about mover composition, but similarity is evidence of robustness only when the HSR estimate is itself sufficiently precise.

Formal identification need not imply informative estimation. When bidirectional support is sparse, ϕ

may be identified from a small or highly concentrated set of trajectories. Researchers should therefore report the amount and concentration of residual support alongside the HSR estimate. If little or no global support remains, the appropriate conclusion is not that path dependence is absent, but that the observed panel cannot distinguish a common path response from unrestricted stable heterogeneity in current-state responses.

5.1. Statistical identification versus causal interpretation

These results concern parameterization, projection, and statistical identification within the maintained state–total-movement model. A causal interpretation of ϕ requires additional assumptions about longitudinal exposure histories, including well-defined interventions and appropriate consistency, interference, and exogeneity conditions (Hernán and Robins 2020; Morgan and Winship 2015). Neither fixed effects nor bidirectional support resolves time-varying confounding, anticipation, endogenous transition timing, or treatment–confounder feedback (Allison 2009; Imai and Kim 2019); nor does bidirectionality by itself make the histories supplying identification representative of a target population. If path responses themselves vary across individuals, the estimand is generally weighted toward trajectories supplying residual bidirectional variation rather than an unconditional population-average path response. Section D of the Online Supplement develops the corresponding potential-outcome formulation and heterogeneous-ϕ_i extension.

6. Monte Carlo Evidence

The simulations address two questions. First, can the pooled asymmetric estimator increasingly reject symmetry as sample size grows even when every individual's response is reversible? Second, when a genuine common path response exists, can relaxing the common-state-response restriction recover that effect, and how does bidirectional support affect precision? Full data-generating processes, analytic population targets, and numerical results appear in Sections B and E of the Online Supplement and the replication archive.

The main experiments use balanced six-wave panels with a binary predictor and outcomes generated from

$$Y_{it} = \alpha_i + \lambda_t + \theta_i X_{it} + \phi V_{it} + \epsilon_{it},$$

where $\alpha_i \sim N(0, 1)$, $\epsilon_{it} \sim N(0, 0.5^2)$, and period effects increase linearly from zero to 0.1. Individuals follow one of six trajectories: always 0, always 1, upward only, downward only, upward then downward, or downward then upward. If q_B denotes the share assigned to the two bidirectional trajectories, 20 percent of the sample is stable, q_B is divided equally between the two bidirectional trajectories, and the remainder is divided equally between upward-only and downward-only movers. The pooled estimator imposes a common current-state response; HSR absorbs an individual-specific current-state response while retaining a common path response. The Online Supplement gives the complete estimation and inference details and derives the exact pooled population targets for this trajectory mixture.

6.1. More data can strengthen spurious asymmetry

The first experiment sets the true path response to zero, $\phi = 0$, while introducing moderate mover composition. Upward-only movers have mean $\theta_i = 1.625$, downward-only movers have mean $\theta_i = 1.375$, and 10 percent of individuals follow bidirectional trajectories. The exact population projection implies a pseudo-true pooled path response of 0.055 even though $\phi_i = 0$ for every individual.

As sample size increases, the pooled estimator becomes more precise around this nonzero target. Figure 2 shows that rejection of $H_0 : \phi = 0$ at 0.05 levels rises from 17.4 percent at $N = 250$ to 56.6 percent at $N = 1{,}000$, 93.0 percent at $N = 2{,}500$, and 99.7 percent at $N = 5{,}000$. By contrast, HSR remains centered near zero, with rejection rates at or below the nominal level. Complete results appear in Table S2 of the Online Supplement.

The result distinguishes an estimand problem from sampling uncertainty. Increasing N does not move the pooled coefficient toward zero because it is not its probability limit under mover composition; instead, more observations tighten the sampling distribution around the nonzero population projection. Larger samples

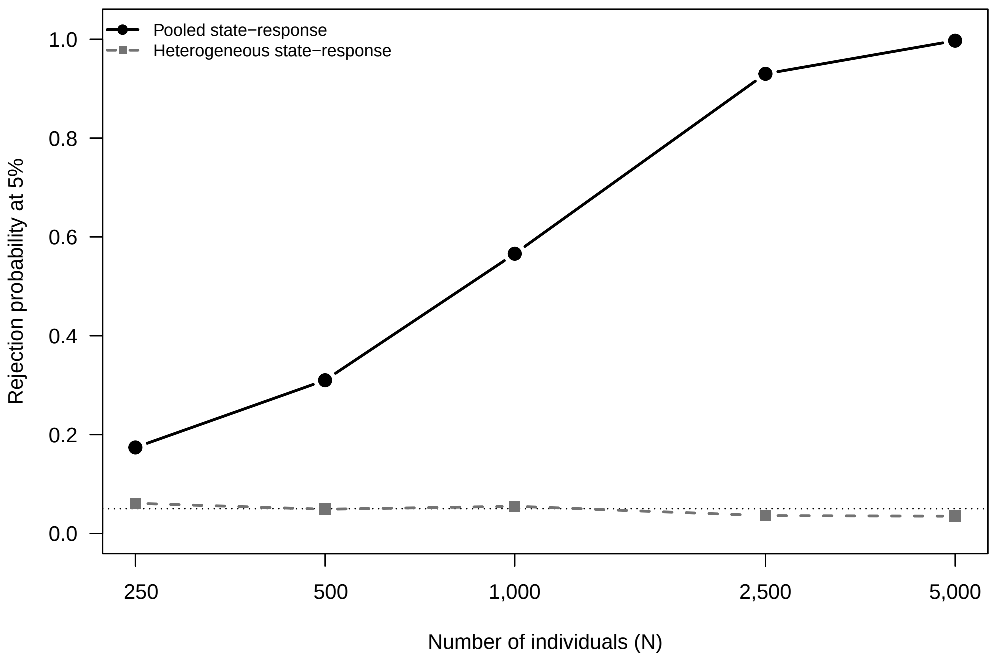

Figure 2: Rejection of $H_0 : \phi = 0$ under universal individual-level reversibility

Note: The horizontal axis reports the number of individuals N on a logarithmic scale, and the vertical axis reports the proportion of Monte Carlo replications rejecting $H_0 : \phi = 0$ at the .05 level. The solid series is the pooled estimator and the dashed series is the heterogeneous-state-response estimator. The true path response is $\phi = 0$, upward-only movers have mean $\theta_i = 1.625$, downward-only movers have mean $\theta_i = 1.375$, and $q_B = 0.1$. Each sample-size cell contains 1,000 Monte Carlo replications. Tests use individual-clustered covariance estimates with t_{G-1} critical values. The horizontal dotted line marks the nominal 0.05 rejection rate.

can therefore strengthen confidence in an incorrect individual-level interpretation of pooled asymmetry.

6.2. Relaxing state-response homogeneity: recovery and precision

The second experiment introduces a genuine common path response and increases the mean-state-response difference between upward-only and downward-only movers to one unit. With 10 percent bidirectional histories, the pooled population target is $\phi + 0.222$. Monte Carlo means closely track this displacement, whereas HSR tracks the true path response: its means are 0.000, 0.251, 0.499, and 0.751 when the true values are 0, 0.25, 0.50, and 0.75, with 95 percent interval coverage between 0.943 and 0.952. The common displacement is the analytically implied mover-composition term for this trajectory design; Section B of the Online Supplement gives the closed-form calculation.

Panel A of Figure 3 illustrates this recovery. Panel B varies bidirectional support while holding $\phi = 0.50$. HSR remains approximately unbiased as q_B increases from 1 percent to 40 percent, while its empirical standard deviation falls from 0.085 to 0.020. At 1 percent support—roughly ten bidirectional respondents in samples of 1,000—cluster-robust intervals undercover despite formal rank identification; from 2.5 percent onward, coverage is within Monte Carlo noise of the nominal level. Thus relaxing state-response homogeneity removes mover composition when the common-ϕ model is correct, but inference becomes fragile when the bidirectional variation identifying ϕ is sparse. Complete results appear in Tables S3–S4.

The other side of the trade-off appears when the common-state-response restriction is correct. As

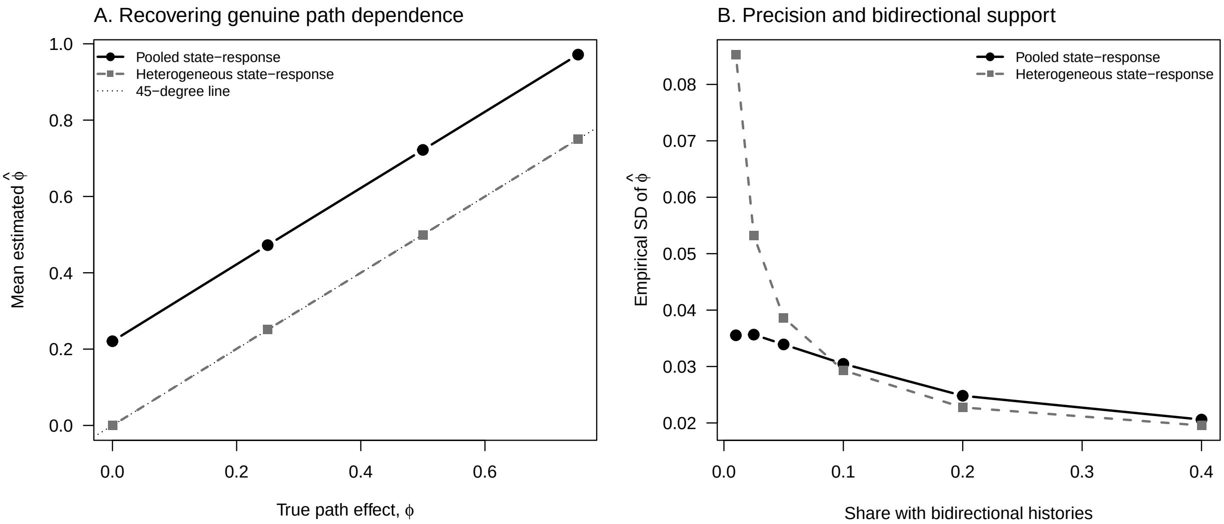

Figure 3: Recovery of path responses and precision under varying bidirectional support

Note: In Panel A, the horizontal axis is the true path response ϕ and the vertical axis is the Monte Carlo mean of $\hat{\phi}$; the dotted 45-degree line marks equality between the true and estimated path responses. The design uses $N = 1{,}000$, $q_B = .10$, a one-unit difference in mean θ_i between upward-only and downward-only movers, and 1,000 replications per value of ϕ. In Panel B, the horizontal axis is the bidirectional share q_B and the vertical axis is the empirical standard deviation of $\hat{\phi}$ across 5,000 replications at each support level, with true $\phi = 0.50$. Solid and dashed series denote the pooled and heterogeneous-state-response estimators, respectively.

Section E.5 of the Online Supplement shows, in that benchmark, both estimators remain centered on the true path response, but HSR is substantially less precise when bidirectional support is sparse. At 1 percent support, its empirical standard deviation is 2.74 times that of the pooled estimator, falling to 1.38 at 5 percent, 1.05 at 20 percent, and approximately one at 40 percent. Additional negative-control simulations confirm that response heterogeneity alone does not create the pooled distortion when it is unrelated to directional histories (see Section E.6 of the Online Supplement). Together, the experiments characterize the assumption–support–precision trade-off: relaxing state-response homogeneity protects against mover composition, but can be costly when the restriction is correct and the histories needed for within-person separation are rare.

7. Empirical Illustration: Reanalyzing Allison's (2019) Wage Example

Allison's (2019) five-wave wage example provides a useful illustration because it contains many transitions in both directions while allowing those transitions to be traced to individual respondents. The sample includes 1,134 respondents observed annually from 1983 through 1987, at ages 18 through 22. The outcome is logged hourly wage, and the time-varying predictors are marital status, years of education, and urban residence. Its original specification allows marriage and urban changes to have different coefficients by direction, while education—which only increases—enters with a single change coefficient. I reproduce that specification, reexpress the asymmetric marriage and urban terms in state–path form, focus on the marital path response, audit the trajectories supporting its identification, and then relax the common current-marriage response. Section F of the Online Supplement gives the full replication, model equations, support diagnostics, sensitivity analyses, and implementation details.

Let M_{it} denote marital status, U_{it} urban residence, and E_{it} years of education, and let V_{it}^M and V_{it}^U denote total movement in marriage and urban residence. The focal heterogeneous-state-response specification is

$$Y_{it} = \alpha_i + \lambda_t + \theta_{iM} M_{it} + \phi_M V_{it}^M + \theta_U U_{it} + \phi_U V_{it}^U + \gamma E_{it} + \epsilon_{it}, \tag{14}$$

where Y_{it} is log hourly wage. Equation (14) allows the current-marriage response θ_{iM} to vary across individuals, while the current urban-residence response θ_U remains common. The corresponding pooled state–path model imposes the additional restriction $\theta_{iM} = \theta_M$ for all individuals. Education enters with a common coefficient because it changes only upward in these data, and the marital and urban path responses remain common in both specifications. All models use the same 1,134 respondents and include individual and period effects. The focal parameter reported below is the marital path response ϕ_M. A stronger sensitivity specification that also allows the current urban-residence response to vary across individuals replaces θ_U with

Table 1: Directional support and path estimates in Allison's (2019) wage example

	Count / Estimate	SE	95% CI
Panel A: Marital-status trajectory support			
No transition	763	-	-
Entry only	258	-	-
Exit only	52	-	-
Both directions	61	-	-
Panel B: Marriage path estimates			
Pooled state–path model	−0.018	0.025	[−0.066, 0.031]
HSR: marriage state response heterogeneous	−0.026	0.034	[−0.092, 0.040]

Note: The outcome is log hourly wage. The balanced sample contains 1,134 respondents observed annually from 1983 through 1987, at ages 18 through 22. All Panel B specifications use the same estimation sample and include individual and period effects, a common education coefficient, and the remaining state–path terms corresponding to Allison's (2019) specification. Every estimate in Panel B is the marital path response $\hat{\phi}_M$. The pooled model imposes a common current-marriage response; HSR allows that response to vary by individual. Standard errors are sandwich estimates clustered by respondent, and 95 percent confidence intervals use the same empirical inference convention documented in Section F of the Online Supplement.

θ_{iU} and is reported in the Online Supplement.

The replication reproduces Allison's published coefficients to rounding (see Table S5 in the Online Supplement). Marriage entry is associated with a log-wage change of 0.032 (SE = 0.023), while marriage exit is associated with a change of −0.067 (SE = 0.048). Applying Equation (5) gives $\hat{\theta}_{\text{mar}} = 0.050$ and $\hat{\phi}_{\text{pool}} = -0.018$; direct estimation in state–path form produces identical fitted values.

The central question is where that directional information comes from. The sample contains 324 marriage entries and 117 exits, but these 441 transitions are distributed unevenly across respondents. As Panel A of Table 1 shows, 763 individuals never change marital status, 258 enter but never exit, 52 exit but never enter, and only 61 move in both directions. Those 61 respondents contribute 66 entries and 65 exits.

Once the common-state-response restriction is relaxed, this distribution matters directly. Entry-only and exit-only respondents contribute to the pooled model because their changes are linked through a common current-marriage response. With individual-specific marriage responses, however, a unidirectional marital history cannot separately identify the current-state and path responses. Direct within-person separation is therefore concentrated among the 61 respondents observed moving in both directions. Because the HSR specification relies on this relatively small set of respondents, its precision—and, under heterogeneous path responses, its implicit weighting—depends on those trajectories.

Panel B of Table 1 shows the corresponding path estimates. The pooled model gives $\hat{\phi}_{\text{pool}} = -0.018$ (SE = 0.025). Allowing the current-marriage response to vary by individual gives $\hat{\phi}_{\text{HSR}} = -0.026$ (SE = 0.034). The comparison therefore illustrates how the source of identifying information changes when the common-state-response restriction is relaxed. In the pooled model, directional information is assembled across respondents under a common current-marriage response; in the HSR specification, separation of the state and path responses relies much more heavily on respondents observed moving in both directions.[3]

The empirical illustration also makes the support distinction concrete. The data contain hundreds of marriage entries and exits, but only a much smaller number of respondents contribute both directions within the same response function once cross-person comparability is relaxed. Thus, abundant directional transitions need not imply abundant within-person information about reversibility.

8. Discussion

Asymmetric FE models combine two appealing features: they exploit within-person change while allowing increases and decreases in a predictor to have different associations with the outcome. This study shows that these features do not, by themselves, make the directional contrast a within-person comparison of reversibility. The key distinction is between what the pooled asymmetric FE model parameterizes and what remains identifiable once the people supplying opposite directions are not assumed to share the same current-state response.

The state–total-movement representation answers the first question without changing the estimator. Allison's cumulative model is exactly equivalent to a model with a current-state response and a path response associated with total movement. Under a common state response, ϕ captures whether accumulated movement matters after current X is held fixed. When current-state responses vary across individuals, however, the pooled path response can combine genuine path dependence with differences in the response functions of the people supplying upward and downward movements. In the two-wave binary case, pooled directional asymmetry can therefore arise even when $\phi_i = 0$ for every individual.

The HSR specification addresses the second question by treating each individual's stable current-state response as an unrestricted nuisance parameter while retaining a common path response. Once those slopes are absorbed, identification depends on trajectories containing movement in both directions: within-person reversals can cancel the same stable state response, whereas cross-person directional contrasts retain differences in state responses. More generally, absolute change contains residual within-person variation if and only if an individual moves in both directions, while global identification additionally requires that this variation survive adjustment for common period effects. With only two waves, that within-person directional separation is unavailable without additional structure.

The pooled and HSR estimators therefore embody an assumption–support–precision trade-off. The pooled model can use unidirectional movers under a common-state-response restriction, which can improve

[3] Sections E–F of the Online Supplement report the additional specification and design-matched inference checks.

precision when bidirectional variation is sparse. HSR protects the path response from mover composition but shifts identification toward richer within-person histories. The Monte Carlo results illustrate both sides: pooled estimates can converge precisely to nonzero path responses under universal individual-level reversibility, whereas HSR removes the composition term but becomes less precise as bidirectional support thins. The reanalysis of Allison's wage example shows how this distinction appears in practice. The data contain many marital transitions in both directions, but a much smaller subset of respondents contributes both directions within the same response function once the common-state-response restriction is relaxed. The example therefore highlights the difference between abundant directional variation in the sample and the more specific within-person variation required for HSR identification.

This argument complements broader work on slope heterogeneity in asymmetric panel models. Most relevant here, Thombs et al. (2022) examine how slope heterogeneity and dynamic misspecification affect estimates of directional asymmetry and motivate heterogeneous-panel approaches in large-N, large-T settings. The present analysis focuses on a distinct problem that arises when directional asymmetry is interpreted as evidence about individual-level reversibility: how heterogeneous state responses interact with the directional histories supplying the pooled contrast. The resulting issue is therefore not slope heterogeneity alone, but whether upward and downward movements are linked within comparable response functions.

The analysis also has clear boundaries. The path response considered here captures dependence on total movement, not unrestricted history dependence: timing, duration, ordering, and decay may matter even when endpoint and total movement are held fixed (Allison 2019). HSR allows stable heterogeneity in current-state responses, not arbitrary time-varying response functions, and neither fixed effects nor bidirectional support resolves time-varying confounding, anticipation, measurement error, endogenous transition timing, or treatment–confounder feedback. Measurement error deserves particular caution because an isolated misclassification can mechanically create apparent bidirectional support, so support audits should examine whether the histories carrying the residual variation are substantively credible. Finally, if path responses vary across individuals, the residualized estimator generally targets a support- and design-dependent average rather than an unconditional population mean; Section D of the Online Supplement develops this extension. The analysis is confined to linear additive panel models; extensions to generalized linear or other nonlinear asymmetric fixed-effects models remain for future work.

Several extensions follow naturally. Richer history summaries could allow path responses to decay or depend on timing and sequence. Partial pooling of individual state responses may provide a useful intermediate specification when common slopes are implausible but bidirectional support is sparse. The same support logic may also extend beyond linear cumulative models wherever positive and negative movements are pooled across individuals and interpreted as evidence about how the same response process behaves in opposite directions.

The key distinction is that, in asymmetric FE models, “within-person” describes the source of the changes used to estimate each directional coefficient; it does not by itself imply that the contrast between those coefficients compares opposite movements within the same person’s response function. When the substantive claim concerns reversibility—whether a process retraces its consequences when its direction changes—the relevant question is therefore not merely whether both directions appear in the sample, but whether the observed trajectories connect those directions within comparable response functions. The trajectory structure determines whether that distinction can be resolved from the data.

References

Allison, P. D. (2009). *Fixed Effects Regression Models*. Sage, Thousand Oaks, CA.

Allison, P. D. (2019). Asymmetric Fixed-Effects Models for Panel Data. *Socius*, 5:1–12. doi:10.1177/2378023119826441.

Arita, S. (2022). Asymmetric Analysis of Panel Data: When and Why Is It Necessary? Panel Survey Discussion Paper Series 152, Institute of Social Science, University of Tokyo, Tokyo.

Clement, M. T. and York, R. (2017). The Asymmetric Environmental Consequences of Population Change: An Exploratory County-Level Study of Land Development in the USA, 2001–2011. *Population and Environment*, 39(1):47–68.

de Chaisemartin, C. and D'Haultfœuille, X. (2020). Two-Way Fixed Effects Estimators with Heterogeneous Treatment Effects. *American Economic Review*, 110(9):2964–2996. doi:10.1257/aer.20181169.

DiPrete, T. A. and Eirich, G. M. (2006). Cumulative Advantage as a Mechanism for Inequality: A Review of Theoretical and Empirical Developments. *Annual Review of Sociology*, 32(1):271–297.

Firebaugh, G., Warner, C., and Massoglia, M. (2013). Fixed Effects, Random Effects, and Hybrid Models for Causal Analysis. In Morgan, S. L., editor, *Handbook of Causal Analysis for Social Research*, pages 113–132. Springer, Dordrecht, the Netherlands. doi:10.1007/978-94-007-6094-3_7.

Frisch, R. and Waugh, F. V. (1933). Partial Time Regressions as Compared with Individual Trends. *Econometrica*, 1(4):387–401.

Gangl, M. (2006). Scar Effects of Unemployment: An Assessment of Institutional Complementarities. *American Sociological Review*, 71(6):986–1013.

Gately, D. and Huntington, H. G. (2002). The Asymmetric Effects of Changes in Price and Income on Energy and Oil Demand. *The Energy Journal*, 23(1):19–55. doi:10.5547/ISSN0195-6574-EJ-Vol23-No1-2.

Halaby, C. N. (2004). Panel Models in Sociological Research: Theory into Practice. *Annual Review of Sociology*, 30:507–544.

Hernán, M. A. and Robins, J. M. (2020). *Causal Inference: What If*. Chapman & Hall/CRC, Boca Raton, FL.

Huang, X. and Jorgenson, A. K. (2018). The Asymmetrical Effects of Economic Development on Consumption-Based and Production-Based Carbon Dioxide Emissions, 1990 to 2014. *Socius*, 4:2378023118773626.

Imai, K. and Kim, I. S. (2019). When Should We Use Unit Fixed Effects Regression Models for Causal Inference with Longitudinal Data? *American Journal of Political Science*, 63(2):467–490.

Lazzari, E. and Beaujouan, É. (2025). Self-assessed Physical and Mental Health and Fertility Expectations of Men and Women Across the Life Course. *Demography*, 62(2):543–569. doi:10.1215/00703370-11873109.

Lieberson, S. (1985). *Making It Count: The Improvement of Social Research and Theory*. University of California Press, Berkeley.

Lovell, M. C. (1963). Seasonal Adjustment of Economic Time Series and Multiple Regression Analysis. *Journal of the American Statistical Association*, 58(304):993–1010.

Mize, T. D. and Kincaid, R. (2025). Role-Accumulation and Mental Health across the Life Course. *American Sociological Review*, 90(2):226–256. doi:10.1177/00031224241313394.

Morgan, S. L. and Winship, C. (2015). *Counterfactuals and Causal Inference: Methods and Principles for Social Research*. Cambridge University Press, New York, 2nd edition.

Rüttenauer, T. and Ludwig, V. (2023). Fixed Effects Individual Slopes: Accounting and Testing for Heterogeneous Effects in Panel Data or Other Multilevel Models. *Sociological Methods & Research*, 52(1):43–84. doi:10.1177/0049124120926211.

Shin, Y., Yu, B., and Greenwood-Nimmo, M. (2014). Modelling Asymmetric Cointegration and Dynamic Multipliers in a Nonlinear ARDL Framework. In Sickles, R. C. and Horrace, W. C., editors, *Festschrift in Honor of Peter Schmidt: Econometric Methods and Applications*, pages 281–314. Springer, New York. doi:10.1007/978-1-4899-8008-3_9.

Sun, Q., Holmqvist Larsson, M., and Falkenström, F. (2021). Separating the Effects of Improvements and Deteriorations in Mechanisms on Outcome Using the Asymmetric Effects Model. *Journal of Counseling Psychology*, 68(6):696–704. doi:10.1037/cou0000569.

Thombs, R. P., Huang, X., and Fitzgerald, J. B. (2022). What Goes Up Might Not Come Down: Modeling Directional Asymmetry with Large-*N*, Large-*T* Data. *Sociological Methodology*, 52(1):1–29. doi:10.1177/00811750211046307.

Thompson, A. J. and Pickett, J. T. (2021). Asymmetry in Process-Based Model Relationships: A Longitudinal Study of Adjudicated Adolescents. *Criminology*, 59(4):585–609. doi:10.1111/1745-9125.12279.

Uccheddu, D., Gauthier, A. H., Steverink, N., and Emery, T. (2019). The Pains and Reliefs of the Transitions into and out of Spousal Caregiving: A Cross-National Comparison of the Health Consequences of Caregiving by Gender. *Social Science & Medicine*, 240:112517. doi:10.1016/j.socscimed.2019.112517.

Western, B. (2002). The Impact of Incarceration on Wage Mobility and Inequality. *American Sociological Review*, 67(4):526–546.

York, R. (2012). Asymmetric Effects of Economic Growth and Decline on CO_2 Emissions. *Nature Climate Change*, 2(11):762–764. doi:10.1038/nclimate1699.

York, R. and Light, R. (2017). Directional Asymmetry in Sociological Analyses. *Socius*, 3:2378023117697180. doi:10.1177/2378023117697180.

ONLINE SUPPLEMENT

When Are Asymmetric Fixed-Effects Models Within-Person Tests of Reversibility? Heterogeneous Responses and Bidirectional Support

This online supplement provides technical derivations, full numerical results, and implementation details for claims developed in the main manuscript. Section A gives the exact state–path reparameterization. Section B derives the general multiperiod pooled estimand and the analytic targets used in the Monte Carlo designs. Section C proves the bidirectional-support result and develops the global rank condition with period effects. Section D gives the potential-outcome interpretation and the extension to heterogeneous path responses. Section E reports the Monte Carlo design and full numerical results underlying the main-text figures and benchmarks. Section F documents the Allison wage replication, support diagnostics, sensitivity checks, and HSR implementation. Notation follows the main text: Y_{it} is the outcome, X_{it} is the time-varying predictor, Δ denotes adjacent-wave first differences, Z_{it}^{+} and Z_{it}^{-} are cumulative positive and negative changes, $V_{it} = Z_{it}^{+} + Z_{it}^{-}$ is total movement, and α_i, λ_t, and ϵ_{it} denote unit, period, and idiosyncratic error components.

A. Exact State–Path Reparameterization

For any scalar increment ΔX_{it}, define

$$\Delta X_{it}^{+} = \max(\Delta X_{it}, 0), \qquad \Delta X_{it}^{-} = \max(-\Delta X_{it}, 0).$$

Then

$$\Delta X_{it} = \Delta X_{it}^{+} - \Delta X_{it}^{-}, \qquad |\Delta X_{it}| = \Delta X_{it}^{+} + \Delta X_{it}^{-}.$$

Summing from $s = 2$ through t gives the cumulative quantities, with the empty-sum convention $Z_{i1}^{+} = Z_{i1}^{-} \equiv 0$:

$$D_{it} = Z_{it}^{+} - Z_{it}^{-} = \sum_{s=2}^{t} \Delta X_{is} = X_{it} - X_{i1}$$

and

$$Z_{it}^{+} + Z_{it}^{-} = \sum_{s=2}^{t} |\Delta X_{is}| = V_{it}.$$

Thus $V_{i1} \equiv 0$ under the same empty-sum convention. Consequently,

$$Z_{it}^{+} = \frac{V_{it} + D_{it}}{2}, \qquad Z_{it}^{-} = \frac{V_{it} - D_{it}}{2}.$$

Substituting into the cumulative asymmetric component yields

$$\begin{aligned} \beta_{+} Z_{it}^{+} + \beta_{-} Z_{it}^{-} &= \frac{\beta_{+} + \beta_{-}}{2} V_{it} + \frac{\beta_{+} - \beta_{-}}{2} (X_{it} - X_{i1}) \\ &= \phi V_{it} + \theta X_{it} - \theta X_{i1}, \end{aligned}$$

where

$$\theta = \frac{\beta_{+} - \beta_{-}}{2}, \qquad \phi = \frac{\beta_{+} + \beta_{-}}{2}.$$

Because X_{i1} is time invariant, $-\theta X_{i1}$ is absorbed into the unit fixed effect. The cumulative directional model and the state–path model therefore have identical fitted values. The inverse transformation is

$$\beta_{+} = \theta + \phi, \qquad \beta_{-} = -\theta + \phi.$$

B. General Multiperiod Pooled Estimand under Heterogeneous Responses

The two-wave binary decomposition in the main manuscript has a direct multiperiod analogue. After any common period components have been removed, write individual i's transformed outcome vector as

$$\mathbf{y}_i = \mathbf{Q}_i \mathbf{b}_i + \mathbf{u}_i, \qquad \mathbf{b}_i = (\theta_i, \phi_i)'.$$

Here $\mathbf{Q}_i$ contains the transformed current-state and total-movement regressors associated with individual i's realized trajectory, and $\mathbf{u}_i$ is the corresponding transformed error vector.

Consider estimating a common coefficient vector $\mathbf{b}$ by minimizing the population weighted least-squares criterion

$$E\left[(\mathbf{y}_i - \mathbf{Q}_i \mathbf{b})' W_i (\mathbf{y}_i - \mathbf{Q}_i \mathbf{b})\right],$$

where W_i is a symmetric positive-definite weighting matrix. Let $\mathbf{b}^*$ denote the population minimizer of this criterion, that is, the pooled population coefficient vector under the common-slope specification. Its first-order condition is

$$E\left[\mathbf{Q}_i' W_i (\mathbf{y}_i - \mathbf{Q}_i \mathbf{b}^*)\right] = 0,$$

or equivalently,

$$E(\mathbf{Q}_i' W_i \mathbf{Q}_i)\mathbf{b}^* = E(\mathbf{Q}_i' W_i \mathbf{y}_i).$$

Substituting $\mathbf{y}_i = \mathbf{Q}_i \mathbf{b}_i + \mathbf{u}_i$ gives

$$E(\mathbf{Q}_i' W_i \mathbf{Q}_i)\mathbf{b}^* = E(\mathbf{Q}_i' W_i \mathbf{Q}_i \mathbf{b}_i) + E(\mathbf{Q}_i' W_i \mathbf{u}_i).$$

Under the orthogonality condition

$$E(\mathbf{Q}_i' W_i \mathbf{u}_i) = 0,$$

and provided that $E(\mathbf{Q}_i' W_i \mathbf{Q}_i)$ is nonsingular,

$$\mathbf{b}^* = \left[E(\mathbf{Q}_i' W_i \mathbf{Q}_i)\right]^{-1} E(\mathbf{Q}_i' W_i \mathbf{Q}_i \mathbf{b}_i). \tag{1}$$

Equation (1) shows that the pooled coefficients are generally design-weighted projections rather than simple population averages of (θ_i, ϕ_i). To make this distinction explicit, define

$$\mathbf{H}_i = \mathbf{Q}_i' W_i \mathbf{Q}_i.$$

If $\mathbf{H}_i$ is mean-independent of $\mathbf{b}_i$, so that

$$E(\mathbf{H}_i\mathbf{b}_i) = E(\mathbf{H}_i)E(\mathbf{b}_i),$$

then Equation (1) reduces to

$$\mathbf{b}^* = E(\mathbf{b}_i).$$

In general, however, this factorization need not hold. The matrix $\mathbf{H}_i$ depends on the direction, magnitude, timing, and frequency of each individual's movements. When these trajectory features are associated with response heterogeneity, individuals with different response parameters contribute differently to the pooled estimand. The realized movement process therefore determines how heterogeneous state and path responses enter the common pooled coefficients.

B.1. Analytic population targets for the Monte Carlo designs

To obtain analytic benchmarks for the Monte Carlo experiments in Section E, this subsection specializes the general pooled estimand in Equation (1) to the six-class trajectory mixture used in those experiments. Let q_B denote the total probability assigned to the two bidirectional classes. The two stable classes each have probability 0.10, the upward-only and downward-only classes each have probability $(0.80 - q_B)/2$, and the two bidirectional classes each have probability $q_B/2$. Let $\Delta_\theta = E(\theta_i \mid U) - E(\theta_i \mid D)$ denote the difference in mean state responses between the upward-only and downward-only classes. For this finite trajectory mixture, the pooled population projection is

$$\phi^*_{\text{pool}} = \phi + \frac{\Delta_\theta}{2}\,\kappa(q_B), \tag{2}$$

where

$$\kappa(q_B) = \frac{12 - 35q_B + 25q_B^2}{12 + 85q_B - 75q_B^2}. \tag{3}$$

The multiplier is specific to this trajectory mixture and weighting scheme. It maps the trajectory-class difference in mean state responses into the population coefficient implied by the pooled common-slope specification.

For the baseline mixture with $q_B = .10$, $\kappa(.10) = 35/79 \approx .44304$. When $\Delta_\theta = .25$ and $\phi = 0$, the pooled population target is

$$\phi^*_{\text{pool}} = \frac{.25}{2}\frac{35}{79} = .05538.$$

When $\Delta_\theta = 1$, the corresponding target is

$$\phi^*_{\text{pool}} = \phi + .22152.$$

For designs that vary q_B, Equation (2) gives the corresponding population target at each support level. Section E examines the finite-sample behavior of the pooled and HSR estimators around these benchmarks.

C. Bidirectional Support and Global Identification

C.1. Proof of the bidirectional-support result

Let $\mathbf{d}_i$ denote individual i's signed-change vector and let $\mathbf{a}_i = |\mathbf{d}_i|$ elementwise. For a symmetric positive-definite weighting matrix W_i, the weighted residual sum of squares from projecting $\mathbf{a}_i$ on $\mathbf{d}_i$ is

$$w_i(W_i) = \mathbf{a}_i' W_i \mathbf{a}_i - \frac{(\mathbf{a}_i' W_i \mathbf{d}_i)^2}{\mathbf{d}_i' W_i \mathbf{d}_i}. \tag{4}$$

For an individual with no change in X, set $w_i(W_i) = 0$. For $r, s \in \mathbb{R}^{T_i - 1}$, define the weighted inner product $\langle r, s \rangle_{W_i} = r' W_i s$. By the Cauchy–Schwarz inequality under this inner product,

$$(\mathbf{a}_i' W_i \mathbf{d}_i)^2 \leq (\mathbf{a}_i' W_i \mathbf{a}_i)(\mathbf{d}_i' W_i \mathbf{d}_i),$$

so $w_i(W_i) \geq 0$, with equality if and only if $\mathbf{a}_i$ and $\mathbf{d}_i$ are linearly dependent.

Suppose $\mathbf{a}_i = c\mathbf{d}_i$ for some scalar c. For every positive nonzero ΔX_{it}, the equality $|\Delta X_{it}| = c\Delta X_{it}$ requires $c = 1$. For every negative nonzero ΔX_{it}, it requires $c = -1$. A common c therefore exists if and only if all nonzero changes have the same sign. Conversely, when all nonzero changes are positive, $\mathbf{a}_i = \mathbf{d}_i$; when all are negative, $\mathbf{a}_i = -\mathbf{d}_i$. Hence

$$w_i(W_i) > 0$$

if and only if individual i has at least one positive and at least one negative nonzero change. The support condition is therefore invariant to the choice of symmetric positive-definite weighting matrix.

C.2. Identity-weighted closed form

Under identity weighting, define

$$S_i^+ = \sum_{t:\Delta X_{it} > 0} (\Delta X_{it})^2, \qquad S_i^- = \sum_{t:\Delta X_{it} < 0} (\Delta X_{it})^2.$$

Here S_i^+ and S_i^- measure the total squared movement in the positive and negative directions, respectively. Because taking absolute values does not change squared magnitudes,

$$\mathbf{a}_i'\mathbf{a}_i = \mathbf{d}_i'\mathbf{d}_i = S_i^+ + S_i^-,$$

while

$$\mathbf{a}_i'\mathbf{d}_i = S_i^+ - S_i^-,$$

since positive changes contribute $(\Delta X_{it})^2$ to the inner product and negative changes contribute $-(\Delta X_{it})^2$.

Substituting these expressions into Equation (4) gives

$$\begin{aligned} w_i(I) &= (S_i^+ + S_i^-) - \frac{(S_i^+ - S_i^-)^2}{S_i^+ + S_i^-} \\ &= \frac{4S_i^+S_i^-}{S_i^+ + S_i^-}. \end{aligned}$$

Equivalently,

$$w_i(I) = (S_i^+ + S_i^-)\left[1 - \left(\frac{S_i^+ - S_i^-}{S_i^+ + S_i^-}\right)^2\right].$$

This representation separates two features of the trajectory. The term $S_i^+ + S_i^-$ measures the total amount of squared movement, while $(S_i^+ - S_i^-)/(S_i^+ + S_i^-)$ measures directional imbalance. Thus, support increases with the overall amount of movement but is reduced when that movement is concentrated in one direction. For fixed $S_i^+ + S_i^-$, support is maximized when $S_i^+ = S_i^-$ and equals zero when either $S_i^+ = 0$ or $S_i^- = 0$. For binary X, S_i^+ and S_i^- reduce to the numbers of entries and exits, respectively. The relevant within-person support therefore depends not simply on the number of transitions, but on how much movement occurs in both directions within the same individual.

C.3. Global rank with period effects

The preceding results characterize whether an individual's trajectory contains absolute-change variation that is distinguishable from that individual's signed changes. This within-person bidirectional support is necessary for identifying a common path response when the state response is unrestricted across individuals. In the full panel model, however, it is not sufficient: common period effects may absorb the residual absolute-change variation that remains after individual-specific state responses have been removed.

To see this, stack the first-difference equation across individuals and periods as

$$\mathbf{y} = \mathbf{D}\boldsymbol{\delta} + \mathbf{Z}\boldsymbol{\theta} + \phi\mathbf{a} + \mathbf{u},$$

where $\mathbf{D}$ contains period-difference indicators, $\mathbf{Z}$ is a block matrix whose ith individual-slope column contains ΔX_{it} for individual i and zero elsewhere, and $\mathbf{a}$ stacks $|\Delta X_{it}|$. Let

$$\mathbf{A} = [\mathbf{D}, \mathbf{Z}]$$

collect the nuisance regressors consisting of the common period effects and individual-specific signed-change terms. Under weighted least squares with symmetric positive-definite W, define the weighted residual-maker

$$M_A^W = I - \mathbf{A}(\mathbf{A}'W\mathbf{A})^{-}\mathbf{A}'W,$$

where $(\cdot)^{-}$ denotes a generalized inverse when nuisance columns are redundant.

By the Frisch–Waugh–Lovell theorem (Frisch and Waugh 1933; Lovell 1963), the common path response ϕ is identified from the component of $\mathbf{a}$ that remains after projection on the nuisance space spanned by $\mathbf{D}$ and $\mathbf{Z}$. Hence ϕ is identified if and only if

$$\mathbf{a}'WM_A^W\mathbf{a} > 0 \tag{5}$$

Equation (5) is equivalently a requirement that $\mathbf{a}$ not lie entirely in the column span of $[\mathbf{D}, \mathbf{Z}]$. The quantity $\mathbf{a}'WM_A^W\mathbf{a}$ is therefore the weighted residual variation in absolute-change variation after removing both individual-specific signed-change responses and common period effects.

Within-person bidirectionality is necessary for this condition. If no individual moves in both directions, each individual's absolute-change vector is proportional to that individual's signed-change vector, so $\mathbf{a}$ is absorbed by $\mathbf{Z}$. Bidirectionality is not sufficient, however, because residual absolute-change variation may itself follow a pattern that is common across individuals and can therefore be absorbed by $\mathbf{D}$. Thus global identification depends not only on whether individuals reverse direction, but also on how those reversals are distributed across periods and across individuals.

Table S1: Illustrative global-rank designs

Design	N	T	Bidirectional share	Residual variation	Identified?
Two waves: up/down movers	200	2	0.00	0.0	No
All same 0–1–0 reversal	200	3	1.00	0.0	No
Half 0–1–0, half stayers	200	3	0.50	100.0	Yes
All reversers, two timing cohorts	200	4	1.00	0.0	No
All reversers, three timing cohorts	300	6	1.00	155.6	Yes

Note: "Residual variation" is the residual sum of squares $\mathbf{a}'M_A\mathbf{a}$ under identity weighting in the diagnostic designs. The numerical values are scale-specific; the relevant distinction for rank is zero versus positive residual variation.

Table S1 illustrates why bidirectionality and global identification must be distinguished. Two-wave panels have no within-person bidirectional support, and even universal reversal can fail to identify ϕ when the remaining absolute-change pattern is absorbed by period effects. Reversers observed alongside stayers or sufficiently varied reversal timing can instead leave positive residual variation; staggering by itself need not do so.

D. Causal Estimands and Heterogeneous Path Responses

D.1. Potential-outcome interpretation

The results in the main manuscript concern parameterization, projection, and statistical identification. A causal interpretation requires additional assumptions about longitudinal exposure histories. Let $\bar{x}_t = (x_1, \ldots, x_t)$ denote a feasible exposure history and let $Y_{it}(\bar{x}_t)$ denote the potential outcome for individual i at time t under that history (Robins 1986; Rubin 1974). Let $m_{it}(\bar{x}_t) \equiv E[Y_{it}(\bar{x}_t)]$ denote the corresponding individual-specific mean potential outcome, and define total movement under the history as

$$V_t(\bar{x}_t) = \sum_{s=2}^{t} |x_s - x_{s-1}|.$$

An individual-level causal analogue of the state–path model is

$$m_{it}(\bar{x}_t) = \alpha_i + \lambda_t + \theta_i x_t + \phi_i V_t(\bar{x}_t). \tag{6}$$

Equation (6) is a strong history-reduction restriction: the exposure trajectory affects the mean potential outcome only through its endpoint and total movement.

For two feasible histories with the same endpoint but different total movement,

$$m_{it}(\bar{x}_t) - m_{it}(\bar{x}'_t) = \phi_i \left[V_t(\bar{x}_t) - V_t(\bar{x}'_t) \right].$$

Thus, within the maintained history-reduction model, $\phi_i = 0$ means that equal-endpoint histories do not differ in mean potential outcome solely because one contains more total movement. For a simple loop $x \to x + d \to x$ relative to remaining at x, the model-implied loop effect is $2|d|\phi_i$; for binary X, a $0 \to 1 \to 0$ or $1 \to 0 \to 1$ loop has effect $2\phi_i$.

Three objects should be distinguished. First, ϕ_i is an individual response-function parameter under Equation (6). Second, $E(\phi_i)$ is an unconditional target-population average. Third, the conventional pooled asymmetric coefficient is a design-dependent projection and, under heterogeneous state responses, can additionally contain the mover-composition term characterized in the main text and Section B. These objects coincide only under additional homogeneity or comparability restrictions.

A causal interpretation further requires consistency and well-defined exposure histories, an appropriate no-interference condition or explicit interference model, correct specification of the state–total-movement history reduction, and an exogeneity condition sufficient for the chosen estimator (Hernán and Robins 2020; Morgan and Winship 2015). Fixed effects do not remove time-varying confounding, and bidirectional support does not render reversers conditionally exchangeable. The heterogeneous-state-response specification addresses the narrower problem of stable heterogeneity in the response to current state.

D.2. Heterogeneous path responses

The heterogeneous-state-response specification in the main text leaves θ_i unrestricted while maintaining a common path response ϕ. To characterize the estimand when path responses also vary across individuals, consider

$$Y_{it} = \alpha_i + \lambda_t + \theta_i X_{it} + \phi_i V_{it} + \epsilon_{it}. \tag{7}$$

Under Equation (7), first consider the period-adjusted first-difference formulation in which the common period effects are known or have already been removed from the differenced outcome. For individual i, let

$$\mathbf{d}_i = (\Delta X_{i2}, \ldots, \Delta X_{iT_i})', \qquad \mathbf{a}_i = (|\Delta X_{i2}|, \ldots, |\Delta X_{iT_i}|)',$$

and let $\mathbf{y}_i$ denote the corresponding vector of period-adjusted outcome changes. Then

$$\mathbf{y}_i = \theta_i \mathbf{d}_i + \phi_i \mathbf{a}_i + \mathbf{u}_i.$$

Under identity weighting, for individuals with $\mathbf{d}_i \neq \mathbf{0}$, define

$$M_i = I - \mathbf{d}_i(\mathbf{d}_i'\mathbf{d}_i)^{-1}\mathbf{d}_i'.$$

For individuals with no change in X, set the support contribution defined below equal to zero. Because $M_i\mathbf{d}_i = \mathbf{0}$, partialling out the individual-specific state response gives

$$M_i\mathbf{y}_i = \phi_i M_i \mathbf{a}_i + M_i \mathbf{u}_i.$$

Define individual i's residual support by

$$w_i = \mathbf{a}_i' M_i \mathbf{a}_i.$$

As established in Section C, $w_i > 0$ if and only if the observed trajectory contains movement in both directions. Thus the same bidirectional histories that identify a common path response when $\phi_i = \phi$ determine which individual path responses contribute when ϕ_i is heterogeneous.

Suppose

$$E\left(\mathbf{a}_i' M_i \mathbf{u}_i\right) = 0$$

and $E(w_i) > 0$. The probability limit of the pooled residual regression is then

$$\phi^*_{\text{HSR}} = \frac{E(w_i \phi_i)}{E(w_i)}. \tag{8}$$

The heterogeneous-state-response estimator therefore targets a support-weighted average of individual path responses, with greater weight placed on trajectories containing more residual bidirectional variation. Individual-specific state responses θ_i do not enter this estimand because they have been partialled out before the common path response is estimated. The resulting target need not equal the unconditional population average $E(\phi_i)$: individuals without bidirectional support receive zero weight, and the remaining weights depend on the geometry of their observed trajectories.

The first-difference derivation and the equivalent levels implementation classify the same trajectories as having zero or positive direct support. In levels, the individual intercept and current state are treated as nuisance components; after differencing, the intercept disappears, current-state change becomes signed change, and change in total movement becomes absolute change. Thus a trajectory whose total movement is completely absorbed by the individual intercept and current state in levels is also one whose absolute changes are completely absorbed by signed changes after differencing, and conversely. The two implementations therefore encode the same bidirectionality criterion used in Section C.

Equation (8) is exact for the period-adjusted formulation under identity weighting. The corresponding weighted version replaces w_i by $\mathbf{a}_i' W_i M_{d_i}^{W_i} \mathbf{a}_i$. When common period effects are instead estimated jointly from the same panel, the target is more generally the coefficient from the global Frisch–Waugh–Lovell projection after period indicators and individual-specific state responses are partialled out. That estimand remains support- and design-dependent but need not reduce to the scalar-weighted average in Equation (8). Generalizing from either supported target to an unconditional average such as $E(\phi_i)$ therefore requires additional assumptions.

E. Monte Carlo Design and Full Results

This section provides the simulation design and numerical results underlying the Monte Carlo findings summarized in the main manuscript. Section B gives the corresponding analytic pooled targets.

E.1. Design and estimation

All main experiments use six waves and binary X, with trajectory templates

$$
\begin{aligned}
S_0 &= (0,0,0,0,0,0), & S_1 &= (1,1,1,1,1,1), \\
U &= (0,0,0,1,1,1), & D &= (1,1,1,0,0,0), \\
R_{UD} &= (0,0,1,1,0,0), & R_{DU} &= (1,1,0,0,1,1).
\end{aligned}
$$

The stable trajectories S_0 and S_1 each have probability 0.10. If q_B is the total bidirectional share, U and D each have probability $(0.80 - q_B)/2$, while R_{UD} and R_{DU} each have probability $q_B/2$.

Outcomes are generated from

$$
Y_{it} = \alpha_i + \lambda_t + \theta_i X_{it} + \phi V_{it} + \epsilon_{it},
$$

where $\alpha_i \sim N(0,1)$, $\epsilon_{it} \sim N(0, 0.5^2)$, and λ_t increases linearly from zero to .10. Unless otherwise stated, θ_i has standard deviation 0.25 around a trajectory-class-specific mean. The pooled estimator imposes a common current-state response; HSR partials out an individual-specific current-state response before estimating the common path response. Both specifications include individual and period effects.

Inference uses individual-clustered sandwich covariance matrices multiplied by $G/(G-1)$ and t_{G-1} critical values, where G is the number of individuals. Across Tables S2–S4, "Mean" is the Monte Carlo mean of $\hat{\phi}$, "Bias" is its difference from the data-generating ϕ, "Emp. SD" is its across-replication standard deviation, "Mean SE" is the mean reported standard error, "Coverage" is nominal 95 percent interval coverage, and "Reject 0.05" is the rejection rate for $H_0 : \phi = 0$ at 0.05 levels when reported.

E.2. Experiment 1: spurious asymmetry as sample size increases

The true path response is zero, $q_B = 0.10$, and mean θ_i is 1.625 for upward-only movers, 1.375 for downward-only movers, and 1.5 for the remaining classes. Each sample-size cell uses 1,000 replications. Table S2 reports the full results for Experiment 1. The pooled mean approaches the nonzero analytic target as N grows, while HSR remains centered near zero; the rejection rates summarized in main-text Figure 2 appear in the table's final column.

Table S2: Spurious asymmetry and sample size

N	Estimator	Mean	Bias	Emp. SD	Mean SE	Coverage	Reject .05
250	Pooled	.0536	.0536	.0517	.0514	.826	.174
250	HSR	-.0030	-.0030	.0580	.0570	.939	.061
500	Pooled	.0537	.0537	.0362	.0365	.690	.310
500	HSR	-.0015	-.0015	.0406	.0409	.951	.049
1,000	Pooled	.0548	.0548	.0262	.0258	.434	.566
1,000	HSR	-.0001	-.0001	.0293	.0288	.945	.055
2,500	Pooled	.0554	.0554	.0161	.0163	.070	.930
2,500	HSR	.0003	.0003	.0175	.0183	.964	.036
5,000	Pooled	.0554	.0554	.0113	.0115	.003	.997
5,000	HSR	.0006	.0006	.0127	.0130	.965	.035

Note: $q_B = 0.10$, $\phi = 0$, and $\mathrm{SD}(\theta_i) = 0.25$ within trajectory class. Each cell contains 1,000 replications. The analytic pooled target is .05538 (Section B).

E.3. Experiment 2: recovering path responses

Here $N = 1{,}000$, $q_B = 0.10$, mean θ_i is 2 for upward-only movers, 1 for downward-only movers, and 1.5 for the remaining classes, and $\phi \in \{0, 0.25, 0.50, 0.75\}$. Each cell uses 1,000 replications. Table S3 reports the full results for Experiment 2. The pooled estimates display the analytic displacement, whereas HSR tracks the data-generating path response with negligible bias and coverage between 0.943 and 0.952.

Table S3: Recovery of path responses

True ϕ	Estimator	Mean	Bias	Emp. SD	Mean SE	Coverage
0.00	Pooled	.2207	.2207	.0311	.0304	.000
0.00	HSR	-.0001	-.0001	.0301	.0289	.947
0.25	Pooled	.4724	.2224	.0303	.0305	.000
0.25	HSR	.2511	.0011	.0295	.0289	.945
0.50	Pooled	.7220	.2220	.0305	.0305	.000
0.50	HSR	.4995	-.0005	.0294	.0290	.952
0.75	Pooled	.9717	.2217	.0309	.0304	.000
0.75	HSR	.7506	.0006	.0295	.0289	.943

Note: $N = 1{,}000$, $q_B = 0.10$, and $\mathrm{SD}(\theta_i) = 0.25$ within trajectory class. Each cell contains 1,000 replications. The analytic pooled target is $\phi + .22152$ (Section B).

E.4. Experiment 3: amount of bidirectional support

The true $\phi = 0.50$, $N = 1{,}000$, and mean θ_i differs by one unit between upward-only and downward-only movers. Each support cell uses 5,000 replications. Table S4 reports the full results for Experiment 3. HSR remains essentially unbiased as q_B varies, while its empirical standard deviation declines from 0.0853 at $q_B = 0.01$ to 0.0196 at $q_B = 0.40$; the coverage pattern summarized in the main text appears in the table's final column.

Table S4: Bidirectional support, bias, and precision

q_B	Estimator	Mean	Bias	Emp. SD	Mean SE	Coverage
.010	Pooled	.9534	.4534	.0355	.0349	.000
.010	HSR	.4993	-.0007	.0853	.0759	.901
.025	Pooled	.8950	.3950	.0357	.0353	.000
.025	HSR	.4993	-.0007	.0532	.0514	.939
.050	Pooled	.8207	.3207	.0339	.0341	.000
.050	HSR	.4996	-.0004	.0387	.0382	.947
.100	Pooled	.7216	.2216	.0305	.0304	.000
.100	HSR	.4998	-.0002	.0293	.0289	.944
.200	Pooled	.6157	.1157	.0248	.0250	.003
.200	HSR	.5005	.0005	.0227	.0228	.953
.400	Pooled	.5292	.0292	.0206	.0203	.696
.400	HSR	.5001	.0001	.0196	.0192	.945

Note: N = 1,000, ϕ = .50, and SD(θ_i) = .25 within trajectory class. Each support cell contains 5,000 replications.

E.5. Efficiency benchmark when the pooled restriction is correct

For the benchmark summarized in the main text, $\phi = 0.50$ and the mean state response is 1.5 in every trajectory class. One design sets $\theta_i = 1.5$ for all individuals; a second allows $\theta_i \sim N(1.5, .25^2)$ independently of trajectory type. Each support cell uses N = 1,000 and 5,000 replications. Both estimators remain centered on the true path response.

At 1 percent bidirectional support, the HSR empirical standard deviation is 2.74 times that of the

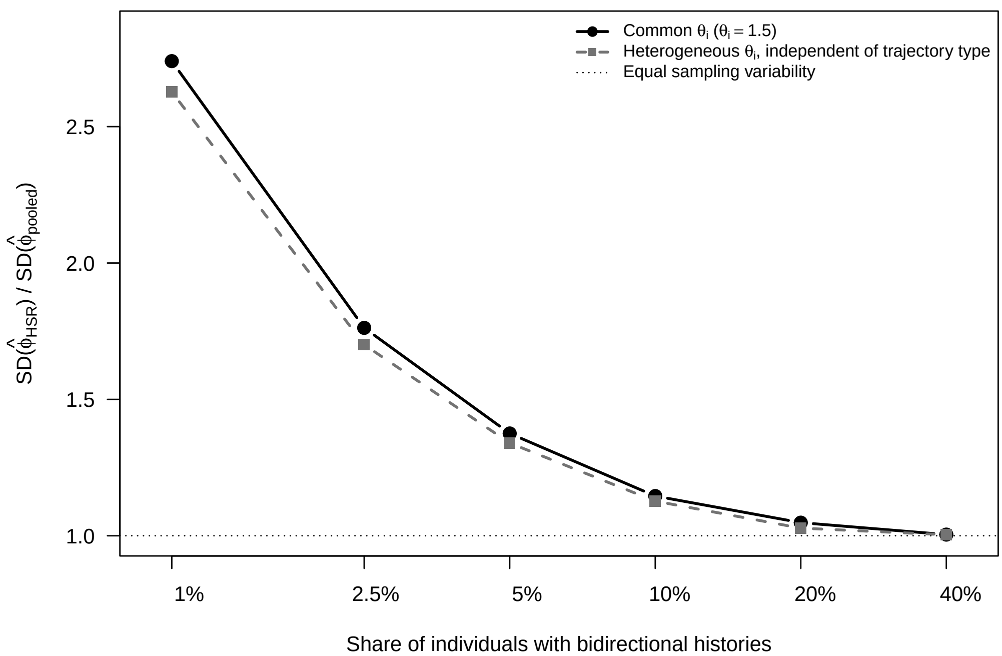

Figure S1: Efficiency of the heterogeneous-state-response estimator when the pooled restriction is correct

Note: The horizontal axis reports q_B on a logarithmic scale. The vertical axis reports $\mathrm{SD}(\hat{\phi}_{\mathrm{HSR}})/\mathrm{SD}(\hat{\phi}_{\mathrm{pooled}})$; values above one indicate greater sampling variability under HSR. The solid series sets $\theta_i = 1.5$ for all individuals, whereas the dashed series allows $\theta_i \sim N(1.5, .25^2)$ independently of trajectory type. Each point summarizes 5,000 replications with N = 1,000 and ϕ = .50.

correctly specified pooled estimator; the ratio falls to 1.38 at 5 percent, 1.05 at 20 percent, and approximately one at 40 percent. Figure S1 displays the complete support grid used for this benchmark.

E.6. Negative-control check

As a negative control, I varied SD(θ_i) from 0 to 1 while holding its mean at 1.5 in every trajectory class, with $\phi = 0$, $N = 1{,}000$, and $q_B = 0.10$. Across the four designs, pooled mean estimates ranged from 0.0010 to 0.0015 and HSR means from −0.0003 to 0.0017. Thus state-response heterogeneity by itself does not generate pooled asymmetry when it is unrelated to directional history. Full cell-level output is included in the replication archive.

F. Allison Wage Replication, Support Audit, and Implementation

This section documents the Allison wage reanalysis summarized in the main manuscript: replication of the original asymmetric specification, additional support diagnostics and a stronger slope-heterogeneity sensitivity, a design-matched inference check, and implementation details.

F.1. Replication and empirical specifications

The illustration uses 1,134 respondents observed annually from 1983 through 1987. The outcome is log hourly wage, and the time-varying predictors are marital status M_{it}, urban residence U_{it}, and years of education E_{it}. There are 4,536 adjacent-wave first differences, including 324 entries into marriage and 117 exits. Education changes only upward.

The focal HSR specification used in the reanalysis is

$$Y_{it} = \alpha_i + \lambda_t + \theta_{iM} M_{it} + \phi_M V_{it}^M + \theta_U U_{it} + \phi_U V_{it}^U + \gamma E_{it} + \epsilon_{it}.$$

The corresponding pooled state–path specification imposes the additional restriction $\theta_{iM} = \theta_M$ for all respondents. The focal HSR specification leaves θ_{iM} unrestricted while retaining a common urban-state response θ_U. The stronger sensitivity additionally allows the current urban-residence response to vary across individuals, replacing θ_U with θ_{iU}. The marital and urban path responses remain common in all specifications. Table S5 verifies the original directional point estimates.[1] The reproduced coefficients agree with Allison's published values to rounding.

[1] Allison's first-difference GLS uses a working covariance matrix with correlation −0.5 between adjacent differences and zero correlation otherwise; its common scale factor does not affect the coefficients. Under this working covariance, the constrained first-difference GLS point estimates are numerically equivalent to the corresponding two-way fixed-effects specification in levels (Wooldridge 2010).

Table S5: Replication of Allison's asymmetric wage coefficients

Parameter	Allison	Replication	Reanalysis SE
Marriage entry	0.032	0.03206	0.02293
Marriage exit	−0.067	−0.06732	0.04788
Education change	0.056	0.05606	0.01573
Urban entry	0.081	0.08155	0.03451
Urban exit	−0.080	−0.08002	0.03621

Note: Allison estimates are from Allison (2019, Table 8, p. 8). "Replication" reproduces the fully constrained GLS point estimates; "Reanalysis SE" gives the respondent-clustered standard error from the equivalent levels representation used in the present analysis. The additional decimal places in the replication column are retained to document numerical reproduction of Allison's estimates.

F.2. Support diagnostics and HSR estimates

Table 1 in the main text reports the marital-status trajectory counts together with the pooled and focal HSR estimates. Table S6 adds the additional slope-heterogeneity sensitivity in which both the marriage and urban current-state responses are heterogeneous and reports diagnostics describing the identifying support under the two HSR specifications.

The 61 respondents observed moving in both marital directions supply the direct within-person separation available to the focal marriage-HSR specification. Before the common-period projection, allowing the urban state response to vary as well reduces the number with positive direct support from 61 to 54. The global rank condition remains satisfied in both specifications, although the residual support is concentrated in a relatively small set of dynamic marital histories.

Table S6: Additional HSR specification and support diagnostics

	Marriage HSR	Marriage + urban HSR
Marriage path estimate, $\hat{\phi}_M$	−0.026	−0.049
SE	0.034	0.035
95% CI	[−0.092, 0.040]	[−0.117, 0.019]
Positive direct within-person support	61	54
Global residual variation, $\mathbf{a}' M_A \mathbf{a}$	183.83	154.09
Share accounted for by top 10 contributors	0.229	0.263

Note: The focal Marriage HSR estimate is repeated from the main-text empirical table only to provide a benchmark for the stronger sensitivity specification. Both specifications use the same 1,134 respondents and include individual and period effects, a common education coefficient, and common marital and urban path responses. The Marriage HSR specification allows only the current-marriage response to vary across respondents; Marriage + urban HSR also allows the current urban-residence response to vary. The 61 bidirectional respondents contribute 66 marriage entries and 65 exits. "Positive direct within-person support" counts respondents whose marital total-movement regressor retains residual variation after removing the individual-specific nuisance slopes and before projecting out common period effects. Global residual variation is the quadratic form entering the full rank condition. The final row reports the share of the squared final residualized path regressor accounted for by the ten largest respondent-level contributors. Inference follows the respondent-clustered convention documented in Section F.3.

F.3. Implementation of the heterogeneous-state-response estimator

For a general linear panel with additional common-slope controls $\mathbf{C}_{it}$, write

$$Y_{it} = \alpha_i + \lambda_t + \theta_i X_{it} + \phi V_{it} + \gamma' \mathbf{C}_{it} + \epsilon_{it}.$$

The HSR specification can be viewed as a fixed-effects individual-slope model in which the current-state response is allowed to vary across individuals. Using the fixed-effects individual-slope (FEIS) residualization logic of Rüttenauer and Ludwig (2023), the individual intercept and state response, (α_i, θ_i), can be partialled out jointly. The analyses here implement this transformation directly using the following Frisch–Waugh–Lovell procedure:

1. For each individual, residualize Y, V, every common-slope control, and the period indicators on $[1, X_i]$.
2. Stack these residuals across individuals.
3. Residualize the transformed Y, V, and controls on the transformed period indicators.
4. Regress the remaining transformed outcome on transformed V and the transformed controls.
5. Conduct inference allowing for repeated observations within individuals.

With multiple individual-specific state responses, replace $[1, X_i]$ in the first step with the corresponding set of state regressors.[2] The individual-specific state slopes are nuisance parameters: their role is to remove from total movement the component that can be represented by stable person-specific current-state responses before estimating the common path response.

[2] For the empirical application in this study, I use respondent-clustered sandwich variance estimates, $\widehat{\mathrm{Var}}(\hat{\beta}) = \frac{G}{G-1} \frac{n_{\mathrm{obs}}-1}{n_{\mathrm{obs}}-k} \widehat{\mathrm{Var}}_{\mathrm{CR0}}(\hat{\beta})$, where G is the number of respondents, n_{obs} is the number of person-wave observations, and k is the number of common-regressor columns in the final residualized regression. Individual intercepts and individual-specific state-response slopes are partialled out before this regression and are not included in k. Reported empirical confidence intervals use the normal critical value 1.96. The main Monte Carlo experiments instead apply only the $G/(G-1)$ correction and use t_{G-1} critical values.

References

Allison, P. D. (2019). Asymmetric Fixed-Effects Models for Panel Data. *Socius*, 5:1–12. doi:10.1177/2378023119826441.

Frisch, R. and Waugh, F. V. (1933). Partial Time Regressions as Compared with Individual Trends. *Econometrica*, 1(4):387–401.

Hernán, M. A. and Robins, J. M. (2020). *Causal Inference: What If.* Chapman & Hall/CRC, Boca Raton, FL.

Lovell, M. C. (1963). Seasonal Adjustment of Economic Time Series and Multiple Regression Analysis. *Journal of the American Statistical Association*, 58(304):993–1010.

Morgan, S. L. and Winship, C. (2015). *Counterfactuals and Causal Inference: Methods and Principles for Social Research.* Cambridge University Press, New York, 2nd edition.

Robins, J. (1986). A new approach to causal inference in mortality studies with a sustained exposure period—application to control of the healthy worker survivor effect. *Mathematical modelling*, 7(9-12):1393–1512.

Rubin, D. B. (1974). Estimating causal effects of treatments in randomized and nonrandomized studies. *Journal of educational Psychology*, 66(5):688.

Rüttenauer, T. and Ludwig, V. (2023). Fixed Effects Individual Slopes: Accounting and Testing for Heterogeneous Effects in Panel Data or Other Multilevel Models. *Sociological Methods & Research*, 52(1):43–84. doi:10.1177/0049124120926211.

Wooldridge, J. M. (2010). *Econometric Analysis of Cross Section and Panel Data.* MIT Press, Cambridge, MA, 2nd edition.